PAPER

Crystalline anisotropy of β-Ga_2O_3 thin films on a c-plane GaN template and a sapphire substrate

To cite this article: Xiaocui Ma *et al* 2022 *Semicond. Sci. Technol.* **37** 035003

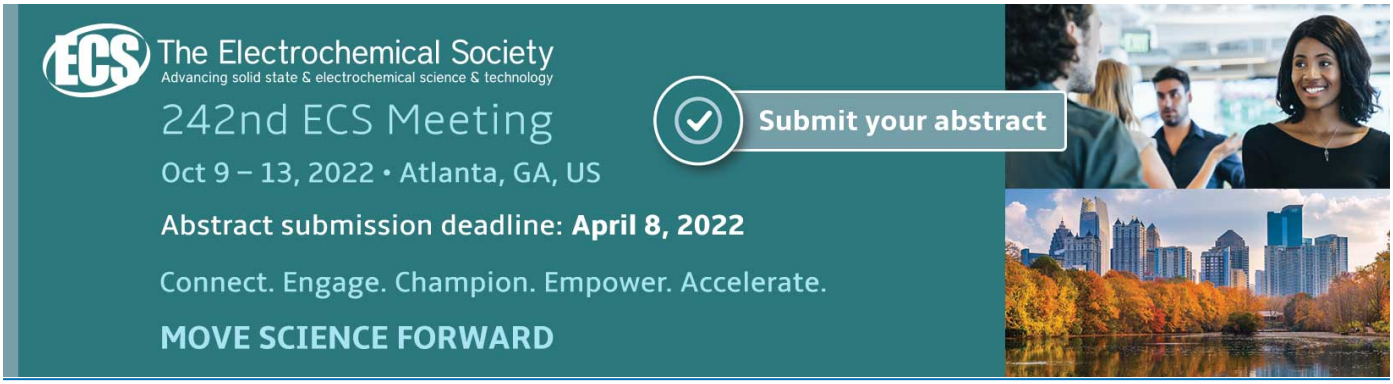

IOP Publishing Semiconductor Science and Technology
Semicond. Sci. Technol. **37** (2022) 035003 (5pp) https://doi.org/10.1088/1361-6641/ac3b3c

Crystalline anisotropy of β-Ga_2O_3 thin films on a c-plane GaN template and a sapphire substrate

Xiaocui Ma, Rui Xu, Yang Mei, Leiying Ying, Baoping Zhang* and Hao Long*

School of Electronic Science and Engineering (National Model Microelectronics College), Xiamen University, Xiamen, Fujian 361005, People's Republic of China

E-mail: bzhang@xmu.edu.cn and longhao@xmu.edu.cn

Received 8 August 2021, revised 4 November 2021
Accepted for publication 17 November 2021
Published 19 January 2022

Abstract

In this work, crystalline anisotropy of heteroepitaxial $(\bar{2}01)$ β-Ga_2O_3 films on a c-plane sapphire substrate and a GaN template was investigated using x-ray diffraction. The $(\bar{2}01)$ ω-scan broadening of β-Ga_2O_3 on GaN exhibited six-fold rotational symmetric anisotropy along different azimuths, with maxima along the [010] direction and minima along the [102] direction, respectively. However, in β-Ga_2O_3 on sapphire, it was nearly isotropic. Smaller lattice mismatch between β-Ga_2O_3 and GaN were taken into account to explain the discrepancy, which also explained the better quality of β-Ga_2O_3 deposited on GaN. Our results present a new viewpoint of the crystallographic anisotropy of $(\bar{2}01)$ β-Ga_2O_3 thin films.

Keywords: anisotropy, β-Ga_2O_3, thin films, XRD, lattice mismatch

(Some figures may appear in color only in the online journal)

1. Introduction

β-gallium oxide (β-Ga_2O_3), with a bandgap of about 4.9 eV [1], was recently extensively studied as an emerging ultrawide bandgap semiconductor. Due to its excellent advantages of mature bulk material's fabrication, superior Baliga's figure of merit, and high electron mobility [2], β-Ga_2O_3 was considered as a promising candidate for solar-blind ultraviolet (UV) photodetectors, gas sensors, UV transparent conductors, and high-power electronic devices [3, 4]. Although bulk β-Ga_2O_3 was an ideal substrate for the epitaxial growth of high-quality β-Ga_2O_3 thin films, its expensive cost and poor thermal conductivity still hindered the commercialization of homoepitaxy. Therefore, heteroepitaxy of β-Ga_2O_3 films on low-cost and large-sized substrates was still important. Many techniques have been employed to grow β-Ga_2O_3 thin films, including molecular beam epitaxy [5], metalorganic chemical vapor deposition (MOCVD) [6], halide vapor phase epitaxy [7], atomic layer deposition, pulse laser deposition [8], and low pressure CVD [9]. Among these methods, MOCVD with controllable growth rate, uniform deposition, and suitability for mass production, became one of the most widely used β-Ga_2O_3 epitaxial technologies.

Recently, heteroepitaxies of β-Ga_2O_3 films on alien Si [10], MgO [11], GaAs [12], GaN [13], and sapphire [14] substrates have been reported. Among them, the growth of $(\bar{2}01)$-oriented β-Ga_2O_3 on (0001) sapphire and (0001) GaN were favored, due to their similar atomic arrangements and small mismatches [15, 16]. Although single crystal β-Ga_2O_3 was two-fold symmetric monoclinic in structure (C_{2h}^3), influenced by the six-fold symmetry of the underneath sapphire or GaN (C_{6v}^4), heteroepitaxial β-Ga_2O_3 thin films typically presented six-fold twins [7, 17]. In 2007, Oshima *et al* [18] observed

* Authors to whom any correspondence should be addressed.

six peaks with 60° intervals in the φ-scans of asymmetric planes of β-Ga_2O_3 on sapphire, which suggested that six-fold twins formed in this single oriented thin film. In 2016, similar six-fold twins were also observed in $(\bar{2}01)$ β-Ga_2O_3 film on a c-plane GaN template by Nakagomi *et al* [19]. The above works all concentrated on the in-plane lattice alignment with the substrate, whereas in-depth understanding of heteroepitaxial β-Ga_2O_3 crystal was rarely reported. Recently, our group found that the rocking curves' (RCs) half-width of $(\bar{2}01)$ bulk β-Ga_2O_3 exhibited two-fold symmetry with azimuth angles [20]. However, the corresponding properties of RCs' symmetry in heteroepitaxial β-Ga_2O_3 layers have not been investigated.

In this work, we investigated the crystalline anisotropies of heteroepitaxial $(\bar{2}01)$ β-Ga_2O_3 films on a c-plane sapphire substrate and a GaN template along different azimuth angles. In general, better crystalline quality was found in β-Ga_2O_3 on the GaN template. Differing from bulk material, the $(\bar{2}01)$ ω-scan broadening of β-Ga_2O_3 on GaN exhibited six-fold rotational symmetric anisotropy with azimuth angles, while β-Ga_2O_3 on sapphire was nearly isotropic. Lattice mismatch and thermal mismatch were taken into account to explain the differences in β-Ga_2O_3 on different substrates. Our results provide some new viewpoints for optimization of β-Ga_2O_3 heteroepitaxial crystal and related devices.

2. Experimental

The β-Ga_2O_3 thin films were deposited using an MOCVD system. Triethylgallium (TEGa) and high-purity (5 N) oxygen gas were used as Ga and oxygen sources, respectively, while 4.5 μm (0001) GaN on sapphire and (0001) sapphire were used as a template and substrate, respectively. The growth temperature and pressure of β-Ga_2O_3 were 800 °C, 40 Torr on GaN and 735 °C, 25 Torr on sapphire, respectively. The thicknesses of β-Ga_2O_3 on GaN and sapphire were 1.8 μm and 2.2 μm, respectively. Bulk $(\bar{2}01)$ oriented β-Ga_2O_3 by edge-defined growth (EFG) was purchased from Tamura Inc. The crystalline structures of thin films were investigated using an x-ray diffractometer (XRD, PANalytical, X Pert PRO) equipped with Cu Kα1 radiation (1.54 Å) with 5 mm × 10 mm irradiation area. Signals were detected by a scintillator detector. Crystalline planes of β-Ga_2O_3 were analyzed by 2θ–ω scans. The epitaxial relationships between β-Ga_2O_3 epilayers and substrates (sapphire and GaN) were determined by φ-scans of skew diffractions. During this measurement, a φ-scan was performed keeping the 2θ and ω angles at respective planes' angles (e.g. the $(\bar{4}22)$ plane of β-Ga_2O_3). Crystalline quality of β-Ga_2O_3 was characterized by ω-scans (RCs) along different azimuth φ angles. Along each φ angle with 10° intervals, the β-Ga_2O_3 $(\bar{2}01)$ plane's ω-scan was performed. The variation of the RCs' width with the φ angle was investigated. The surface morphologies were observed using atomic force microscopy (AFM, Nanonavi, SPA400) in contact scanning mode with 10 μm × 10 μm probing range and scanning electron microscopy (SEM, ZEISS, SIGMA-HD) at 10 kV voltage.

3. Results and discussion

Figure 1(a) displays 2θ–ω scans of β-Ga_2O_3 layers deposited on GaN and sapphire. Relatively broader Bragg peaks were observed at 2θ of 18.95°, 38.40°, 59.19°, 82.37°, and 110.56° in the XRD profiles, which were identified as the $(\bar{2}01)$, $(\bar{4}02)$, $(\bar{6}03)$, $(\bar{8}04)$, and $(\bar{1}0\bar{1}0\bar{5})$ Bragg diffractions of the β-Ga_2O_3 $\{\bar{2}01\}$ family. This observation indicated that our β-Ga_2O_3 layers were purely oriented along the $[\bar{2}01]$ direction. The diffraction intensity of β-Ga_2O_3 on GaN was stronger than that on sapphire, suggesting that β-Ga_2O_3 grown on GaN had better crystal quality. The discrepancies in surface morphology of β-Ga_2O_3 on different substrates were analyzed using SEM and AFM. As presented in figures 1(b) and (c), both β-Ga_2O_3 samples exhibited coarse surficial roughness with closely packed crystal grains. The grain size of β-Ga_2O_3 on GaN was larger than that on sapphire. The root mean square roughness of β-Ga_2O_3 on GaN and sapphire were 16.87 nm and 14.54 nm, respectively. This phenomenon was ascribed to the differences in lattice mismatch, the thermal expansion coefficient (TEC), growth conditions, and the strain release mechanism of β-Ga_2O_3 on different substrates.

To determine the in-plane epitaxial alignment of $(\bar{2}01)$ β-Ga_2O_3 with respect to GaN and sapphire, φ scans were performed on $(\bar{4}22)$ β-Ga_2O_3 and $(10\bar{1}2)$ substrates (GaN and sapphire), respectively, as shown in figures 2(a) and (b). On both substrates, six $(\bar{4}22)$ β-Ga_2O_3 diffraction peaks with 60° intervals were observed, reflecting six-fold twins crystal. In contrast, bulk β-Ga_2O_3 by EFG (figure 2(c)) owned only two $(\bar{4}22)$ β-Ga_2O_3 diffraction peaks separated by 180° due to the monoclinic structure of β-Ga_2O_3. In heteroepitaxy, underlying GaN and sapphire with six-fold symmetry made the β-Ga_2O_3 grow at the same rate along every one of the six crystallographic directions, causing in-plane six-fold rotational symmetry. In β-Ga_2O_3 on GaN, six peaks of $(10\bar{1}2)$ GaN were detected along 30° offset from $(\bar{4}22)$ β-Ga_2O_3, showing alignments of β-Ga_2O_3 [010] ∥ GaN $[10\bar{1}2]$ and β-Ga_2O_3 [102] ∥ GaN $[10\bar{1}1]$. During the growth process, oxygen atoms chemically stuck onto the surficial Ga atoms of GaN and formed a new octahedral Ga-O structure, where the foreign β-Ga_2O_3 layer started to grow. For β-Ga_2O_3 on sapphire, diffraction peaks of the $(\bar{4}22)$ β-Ga_2O_3 plane appeared at the same azimuth angles as $(10\bar{1}2)$ sapphire. The in-plane alignment relationships of β-Ga_2O_3 on sapphire were β-Ga_2O_3 [010] ∥ sapphire $[10\bar{1}0]$ and β-Ga_2O_3 [102] ∥ sapphire $[11\bar{2}0]$. Our results were in line with other groups [17, 21–23].

From the φ-scan results in figure 2, it could be seen that the in-plane rotational symmetries of the $(\bar{2}01)$ β-Ga_2O_3 epilayers were changed from two-fold of bulk one to six-fold due to the underneath GaN and sapphire substrates. To further investigate the six-fold twins in heterogeneous epitaxy, the RCs of $(\bar{2}01)$ β-Ga_2O_3 planes were measured along various azimuth angles (10° intervals), as shown in figure 3(a).

The RC broadenings of β-Ga_2O_3 on GaN presented a six-fold symmetric anisotropy, as seen in figure 3(b). The broadening along the β-Ga_2O_3 [010] direction (i.e. $[11\bar{2}0]$ of GaN) reached a maxima of an average of 2.51°, while it reached a minima of an average of 2.37° along the [102] direction.

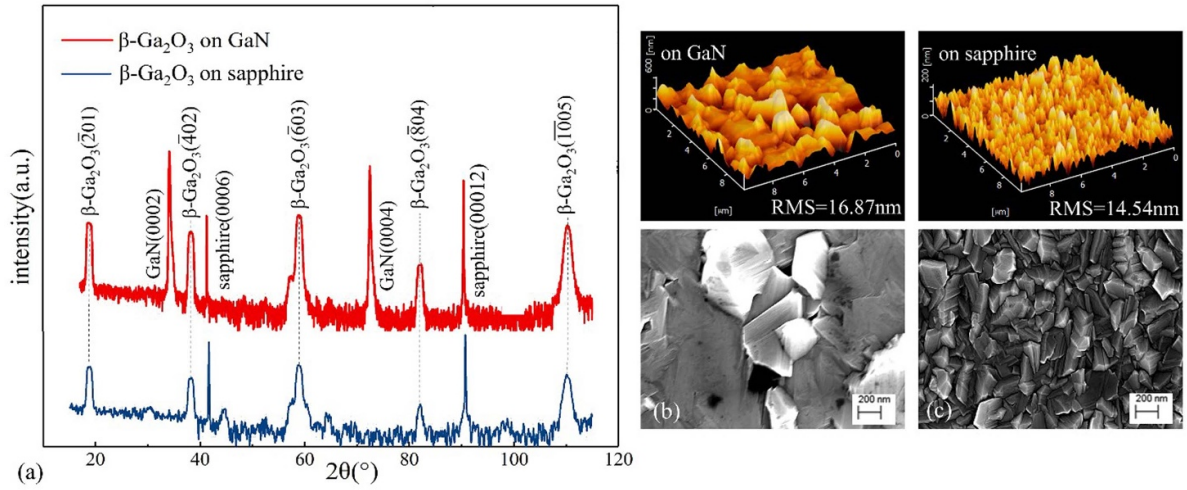

Figure 1. (a) XRD $2\theta-\omega$ scan curves of $(\bar{2}01)$ β-Ga_2O_3 on GaN and sapphire; AFM (10 μm $\times$ 10 μm) and SEM surface images of β-Ga_2O_3 on (b) GaN and (c) sapphire, respectively.

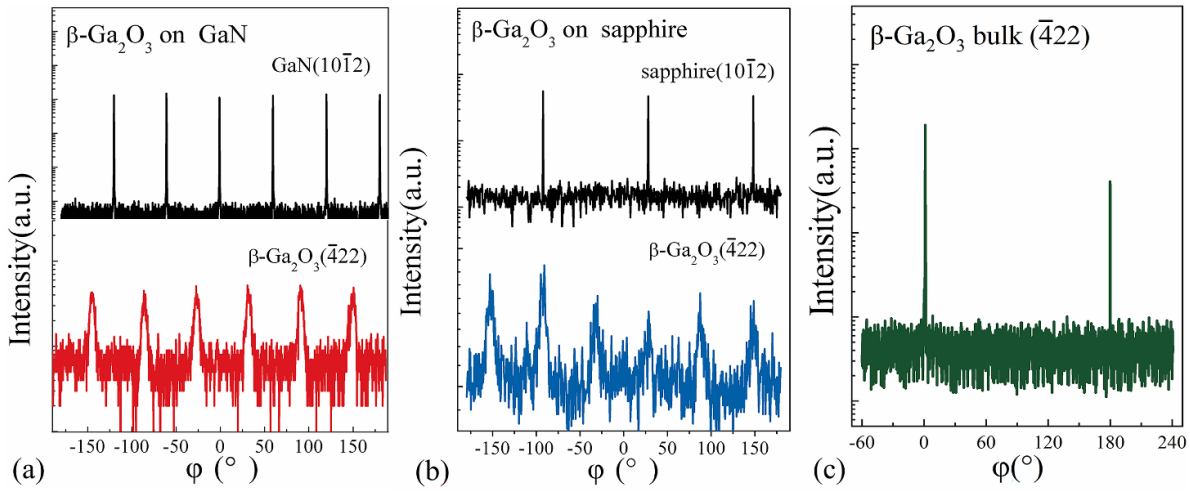

Figure 2. The φ-scans of (a) $(\bar{4}22)$ β-Ga_2O_3 and $(10\bar{1}2)$ GaN planes in β-Ga_2O_3 on GaN; (b) $(\bar{4}22)$ β-Ga_2O_3 and $(10\bar{1}2)$ sapphire planes in β-Ga_2O_3 on sapphire; (c) $(\bar{4}22)$ β-Ga_2O_3 in β-Ga_2O_3 bulk.

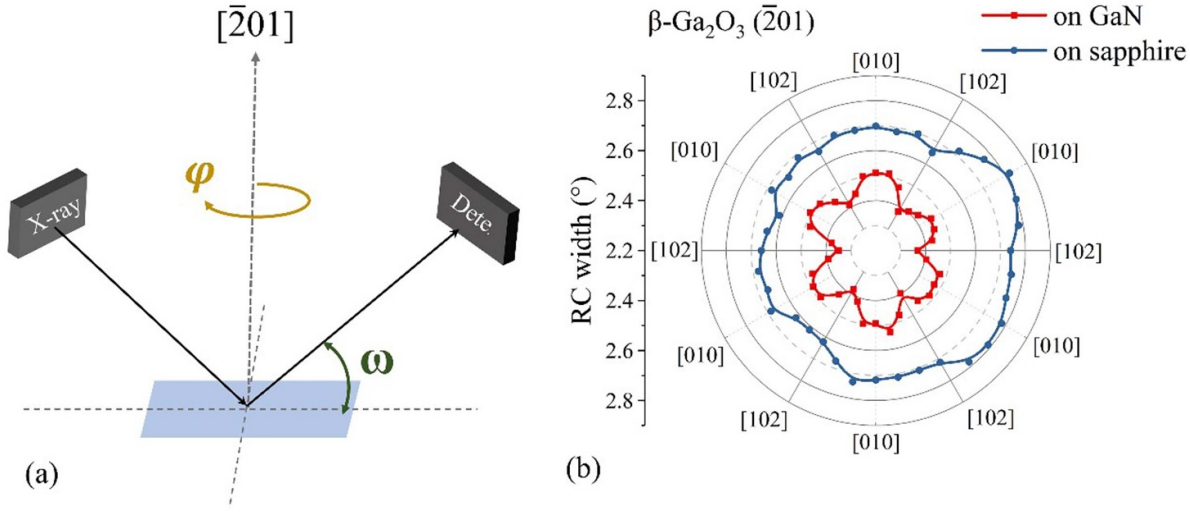

Figure 3. (a) XRD RCs measured along different φ angles; (b) a polar diagram of $(\bar{2}01)$ RC broadening along different azimuths.

Table 1. In-plane lattice mismatch and thermal mismatch between β-Ga_2O_3 on GaN and β-Ga_2O_3 on sapphire.

Sample	Epitaxial relationship	Lattice mismatch	TEC of β-Ga_2O_3 [28] (10^{-6} K^{-1})	TEC of GaN [29] or sapphire [30] (10^{-6} K^{-1})	Thermal mismatch
β-Ga_2O_3 on GaN	[010] ∥ [11$\bar{2}$0]	+4.67%	7.8	5.59	−0.17%
	[102] ∥ [10$\bar{1}$0]	0%	7.02	9.682	+0.21%
β-Ga_2O_3 on sapphire	[010] ∥ [10$\bar{1}$0]	+1.62%	7.8	12.99	+0.37%
	[102] ∥ [11$\bar{2}$0]	−3.12%	7.02	7.5	+0.034%

'+': tensile strain, '−': compressive strain.

In contrast to β-Ga_2O_3 on GaN, β-Ga_2O_3 on sapphire was poorer quality and exhibited larger broadening along all azimuth angles. The quality distinction between β-Ga_2O_3 grown on GaN templates and sapphire substrates was also studied in the work of Zhang *et al* [24–26] and Hao *et al* [27], which confirmed our results. Meanwhile, the broadening of β-Ga_2O_3 on sapphire presented a near-isotropic feature. Both results were different from EFG-grown β-Ga_2O_3 bulk materials, whose RC half-width exhibited two-fold symmetry [20], reported by our previous paper.

The half-width of the ω-scan was an important parameter used to characterize the crystal quality. Due to the differences in lattice mismatch and TECs between the epilayer and substrates, heterogeneous epitaxy inevitably suffered from strains, whose relaxation subsequently caused defects. Therefore, we calculated the lattice mismatch δ and thermal mismatch ε [28] of both samples along the [010] and [102] directions:

$$\delta = \frac{l_{\text{sub}} - l_{\text{Ga2O3}}}{l_{\text{sub}}} \tag{1}$$

$$\varepsilon = \frac{(\alpha_{\text{sub}} - \alpha_{\text{Ga2O3}})\,\Delta T}{1 - \alpha_{\text{sub}}\Delta T} \tag{2}$$

where l was the lattice constant, α was the TEC, ΔT was the temperature difference between epitaxy temperature and room temperature, and sub and Ga_2O_3 represented the substrate and β-Ga_2O_3 layer, respectively. According to the calculated results in table 1, we found that the strain caused by thermal mismatch was relatively small, whose effect on crystal quality was less than that of lattice mismatch. The lattice mismatch value between β-Ga_2O_3 and GaN was 4.67% along the β-Ga_2O_3 [010] direction and near zero along the β-Ga_2O_3 [102] direction, respectively. This large lattice mismatch difference accounted for the obvious anisotropic RC width of β-Ga_2O_3 on GaN. In β-Ga_2O_3 on sapphire, the lattice mismatch values along β-Ga_2O_3 [010] and [102] were 1.62% and 3.12%, respectively. The difference in lattice mismatch between the two directions was smaller than that of β-Ga_2O_3 on GaN, inducing homogeneous defects distribution and isotropic broadening.

Investigation of anisotropy of β-Ga_2O_3 crystalline quality is essential to the fabrication of relative devices. Properties (including: breakdown field, on resistance, transconductance, thermal conductance, etc) of β-Ga_2O_3 metal-oxide-semiconductor field effect transistors will be different along different crystalline orientations [31, 32]. Photo-detectors will have varied responsivities and response times for different polarized light [33, 34]. Therefore, further optimization, design and attenuation of heteroepitaxial β-Ga_2O_3 thin films' crystalline anisotropy could benefit the devices' fabrication and performance.

4. Conclusion

In this work, we investigated the crystalline anisotropy of β-Ga_2O_3 films deposited on a sapphire substrate and a GaN template, respectively. In comparison with sapphire, the lattice mismatch anisotropy between the GaN template and β-Ga_2O_3 along the [010] and [102] directions is larger, causing six-fold anisotropy in broadening. In contrast, the absolute lattice mismatch of β-Ga_2O_3 deposited on sapphire was relatively isotropic along the [010] and [102] directions, making the RC's broadening almost isotropic. Furthermore, the GaN template efficiently improved the crystalline quality of β-Ga_2O_3. Our work will provide a new insight into β-Ga_2O_3's material properties and also benefit the further optimization of heteroepitaxial β-Ga_2O_3 thin films and related devices.

Data availability statement

All data that support the findings of this study are included within the article (and any supplementary files).

Acknowledgments

The work was supported by the National Key Research and Development Program of China (No. 2017YFE0131500), the National Natural Science Foundation of China (No. 62174140), the Natural Science Foundation of Fujian Province of China (No. 2019J05023) and the Youth Innovation Foundation of Xiamen, China (No. 3502Z20206055). The authors are also grateful to Professor Weihua Tang from Beijing University of Posts and Telecommunications for the meaningful discussion.

ORCID iDs

Baoping Zhang https://orcid.org/0000-0001-9537-5179
Hao Long https://orcid.org/0000-0002-7057-7214

References

[1] Matsuzaki K, Hiramatsu H, Nomura K, Yanagi H, Kamiya T, Hirano M and Hosono H 2006 *Thin Solid Films* **496** 37–41
[2] Higashiwaki M, Sasaki K, Kuramata A, Masui T and Yamakoshi S 2012 *Appl. Phys. Lett.* **100** 013504
[3] Pearton S J, Yang J, Cary P H, Ren F, Kim J, Tadjer M J and Mastro M A 2018 *Appl. Phys. Rev.* **5** 011301
[4] Chen X, Ren F, Gu S and Ye J 2019 *Photon. Res.* **7** 381–415
[5] Ghose S, Rahman S, Hong L, Rojas-Ramirez J S, Jin H, Park K, Klie R and Droopad R 2017 *J. Appl. Phys.* **122** 095302
[6] Alema F, Hertog B, Osinsky A, Mukhopadhyay P, Toporkov M and Schoenfeld W V 2017 *J. Cryst. Growth* **475** 77–82
[7] Li Y, Xiu X, Xu W, Zhang L, Xie Z, Tao T, Chen P, Liu B, Zhang R and Zheng Y 2021 *J. Appl. Phys.* **54** 014003
[8] Lee S-A, Hwang J-Y, Kim J-P, Jeong S-Y and Cho C-R 2006 *Appl. Phys. Lett.* **89** 182906
[9] Rafique S, Han L, Neal A T, Mou S, Tadjer M J, French R H and Zhao H 2016 *Appl. Phys. Lett.* **109** 132103
[10] Chen Z, Nishihagi K, Wang X, Saito K, Tanaka T, Nishio M, Arita M and Guo Q 2016 *Appl. Phys. Lett.* **109** 102106
[11] Víllora E G, Shimamura K, Kitamura K and Aoki K 2006 *Appl. Phys. Lett.* **88** 031105
[12] Zaccai G *et al* 2016 *Sci. Rep.* **6** 31434
[13] Ghosh S, Srivastava H, Rao P N, Nand M, Tiwari P, Srivastava A K, Jha S N, Rai S K, Singh S D and Ganguli T 2020 *Semicond. Sci. Technol.* **35** 085024
[14] Oshima T, Arai N, Suzuki N, Ohira S and Fujita S 2008 *Thin Solid Films* **516** 5768–71
[15] Guo D *et al* 2014 *Opt. Mater. Express* **4** 1067
[16] Li W, Zhang X, Meng R, Yan J, Wang J, Li J and Wei T 2019 *Micromachines* **10** 322
[17] Cao Q, He L, Xiao H, Feng X, Lv Y and Ma J 2018 *Mater. Sci. Semicond. Process.* **77** 58–63
[18] Oshima T, Okuno T and Fujita S 2007 *Jpn. J. Appl. Phys.* **46** 7217–20
[19] An Q and Li G 2017 *Phys. Rev.* B **96** 144113
[20] Ma X C, Xu R, Xu J F, Ying L Y, Mei Y, Long H and Zhang B P 2021 *J. Appl. Cryst.* **54** 1153–7
[21] Kalra A, Vura S, Rathkanthiwar S, Muralidharan R, Raghavan S and Nath D N 2018 *Appl. Phys. Express* **11** 064101
[22] Nakagomi S and Kokubun Y 2016 *Phys. Status Solidi* (b) **253** 1217–21
[23] Bosi M, Mazzolini P, Seravalli L and Fornari R 2020 *J. Mater. Chem.* C **8** 10975–92
[24] Zhang Y, Li Y, Wang Z, Guo R, Xu S, Liu C, Zhao S, Zhang J and Hao Y 2020 *Sci. China Phys. Mech. Astron.* **63** 11
[25] Zhang T, Li Y, Zhang Y, Feng Q, Ning J, Zhang C, Zhang J and Hao Y 2021 *J. Alloy Compd.* **859** 157810
[26] Zhang T, Hu Z, Li Y, Zhang Y, Feng Q, Ning J, Zhang C, Zhang J and Hao Y 2021 *J. Lumin.* **233** 117928
[27] Hao S J *et al* 2019 *J. Appl. Phys.* **125** 10
[28] Liao M E, Li C, Yu H M, Rosker E, Tadjer M J, Hobart K D and Goorsky M S 2019 *Apl. Mater.* **7** 022517
[29] Reeber R R and Wang K 2000 *J. Mater. Res.* **15** 40–44
[30] Yim W M and Paff R J 1974 *J. Appl. Phys.* **45** 1456–7
[31] He H, Blanco M A and Pandey R 2006 *Appl. Phys. Lett.* **88** 261904
[32] Guo Z, Verma A, Wu X, Sun F, Hickman A, Masui T, Kuramata A, Higashiwaki M, Jena D and Luo T 2015 *Appl. Phys. Lett.* **106** 111909
[33] Onuma T, Saito S, Sasaki K, Masui T, Yamaguchi T, Honda T and Higashiwaki M 2015 *Jpn. J. Appl. Phys.* **54** 112601
[34] Wang Y *et al* 2018 *Sci. Rep.* **8** 18075